5-2021

Utilizing the oxygen-barrier properties of poly(isobutylene) to enhance photon upconversion in thermoplastic elastomers

Haley Carroll

Utilizing the oxygen-barrier properties of poly(isobutylene) to enhance photon upconversion in thermoplastic elastomers

by

Haley Carroll

A Thesis
Submitted to the Honors College of
The University of Southern Mississippi
in Partial Fulfillment
of Honors Requirements

May 2021

Approved by:

Yoan Simon, Ph.D., Thesis Advisor,
School of Polymer Science and Engineering

Derek Patton, Ph.D., Director,
School of Polymer Science and Engineering

Ellen Weinauer, Ph.D., Dean
Honors College

ABSTRACT

Upconversion (UC) is the conversion of low energy light to higher energy light. It is utilized for a broad range of applications such as solar energy harvesting, microscopy of cellular biology, and cancer therapy. Specifically, triplet-triplet annihilation UC (TTA-UC) involves two dye species, a sensitizer and an annihilator, which are capable of upconverting noncoherent light such as sunlight. Traditionally, TTA-UC is achieved in solution, rubbers, or glasses, however, this work probes the capabilities of a thermoplastic elastomer (TPE) matrix to examine the effect of phase-separated morphology on the energy transfers necessary for TTA-UC. The system herein consists of poly(styrene-isobutylene-styrene) (SIBstar) as the TPE matrix, palladium octaethylporphyrin (PdOEP) as the sensitizer, and diphenyl anthracene (DPA) as the annihilator. Several processing methods (solvent-casting, spin-coating, melt-processing) were explored to incorporate the dyes homogenously within the TPE. However, only low levels of UC were detected in the latter. Assuming aggregation of DPA to be the main hindrance to UC in SIBstar, covalent attachment of DPA to the styrenic portion of the SIBstar backbone was performed. The resulting DPA modified SIBstar (DPAstar) proved unprocessable. While UC was not achievable in these systems, the ability to control and modulate UC through copolymer morphology remains intriguing for the development of flexible, robust, and efficient polymer materials.

Keywords: thermoplastic elastomer, triplet-triplet annihilation, upconversion

DEDICATION

To God, for everything. To my parents, my fiancé Samuel, and loved ones for all of the encouragement and support that allowed me to persevere through a challenging four years.

ACKNOWLEDGMENTS

I would like to acknowledge the mentorship and wisdom of my graduate student, Brad Davis. Thank you for teaching me more than I could have hoped for and providing me with the confidence to move forward to graduate school. Thank you to all of the graduate students in the Simon Research Group for the support and friendship that made my lab experience so enjoyable. I would like to acknowledge Eric King and the Azoulay Research Group for completing the Suzuki coupling reaction. Finally, I would like to thank my advisor, Dr. Yoan Simon, for fostering my skills as a researcher throughout the entirety of my undergraduate career.

TABLE OF CONTENTS

LIST OF ILLUSTRATIONS

LIST OF ABBREVIATIONS

DPA	9,10- diphenylanthracene
DPAstar	Poly(styrene-isobutylene-styrene-DPA)
DSC	Differential scanning calorimetry
ISC	Intersystem crossing
OPV	Organic photovoltaic
PdOEP	Palladium octaethylporphyrin
PIB	Poly(isobutylene)
PS	Poly(styrene)
SIBstar	Poly(styrene-isobutylene-styrene)
Tg	Glass transition temperature (℃)
TGA	Thermogravemetric analysis
Tm	Melting temperature (℃)
TTA	Triplet-triplet annihilation
TTET	Triplet-triplet energy transfer
TWh	Terawatt hour
UC	Upconversion

CHAPTER I: INTRODUCTION

Currently, the world relies heavily on fossil fuels to provide most of its energy. In 2019, U.S. annual energy consumption reached ~29,000 terawatt hour (TWh), and it is predicted for global consumption to increase 50% by 2050.[1] The reliance on non-renewable energy has become increasingly alarming with petroleum stockpiles decreasing. Within the near future, the influence on our planet from such exploitation of non-renewable fossil fuels will cause a decline in the overall environment. Obtaining reliable renewable energy sources is of key importance; wind, hydroelectric, nuclear, and solar energy are viable options for the replacement of petroleum, coal, and natural gas. Solar energy is particularly attractive as a replacement to fossil fuels, as it is the most abundantly available resource that possesses true renewability. For perspective, the sun provides enough energy in one hour to supply the global consumption of energy for an entire year.[2] This makes solar energy a top contender for the focus of future energy production, and in turn, a rising focus for several different areas of research, including polymer science and engineering; this trend is evident in the growth of solar energy consuption from 15 GW in 2008 to 505 GW only ten years later (Figure 1).[3]

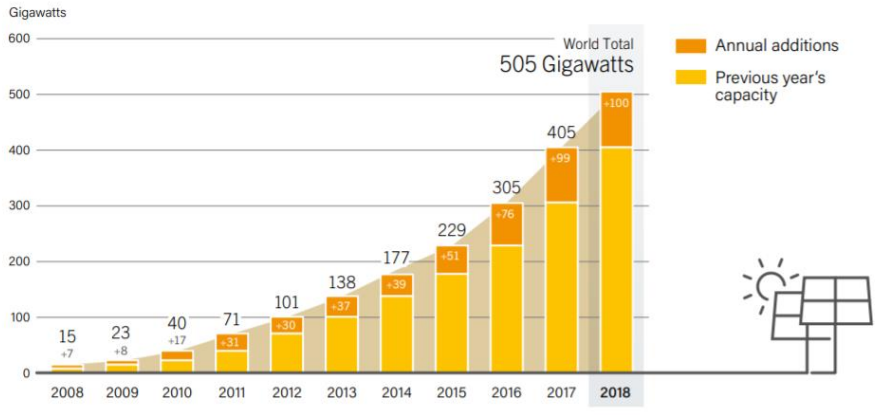

Figure 1. World market for solar photovoltaics from 2008 to 2018.[3]

Polymers can be utilized in an expansive list of applications[4–6], and energy harvesting is no exception. Solar cells have long been produced from inorganic materials which have recently achieved record breaking efficiencies of close to 50%, but organic photovoltaics (OPVs) have begun to compete with their traditional counterparts and are currently being produced with efficiencies of 18% (Figure 2).[7,8] While polymeric solar cells cannot currently match efficiency percentages, polymers possess desirable properties that prove to be more suitable for fabricating solar cells in comparison to inorganic cells, due to their reduction of cost, mechanical flexibility, versatility of design, and ease of integration.[9–11] These properties can provide pathways for OPVs to be exploited in new and advantageous applications like wearable electronics and solar-powered vehicles, for which inorganic materials would not have suitable properties.[12,13]

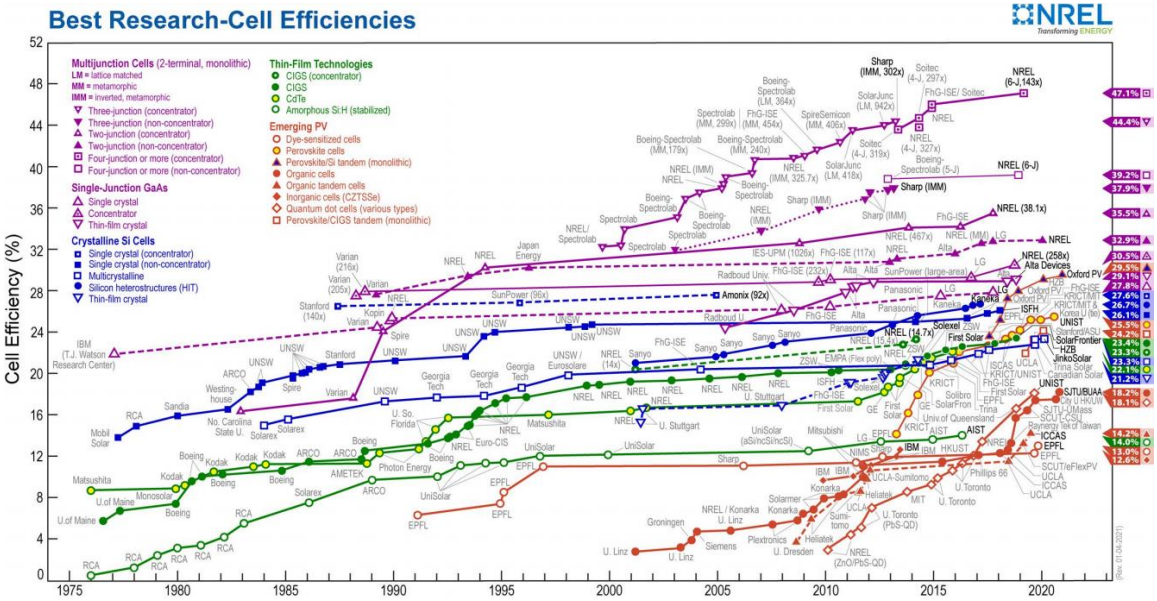

Figure 2. OPVs are shown to have efficiencies of 18% (solid orange circle) while inorganic solar cells have reached as high as 47% (purple square with dot). This plot is courtesy of the National Renewable Energy Laboratory, Golden, CO.[8]

Abundant research efforts have been aimed at direct harvesting of solar energy through photovoltaics,[14–17] but there is limitation to the range of wavelengths that can be utilized for energy. Focus on increasing systems of indirect energy harvesting by methods such as upconversion, later described in detail, can broaden the spectrum of photons available for electricity and thus, there is great potential for increased solar cell efficiencies.[18–20] For example, the range of a traditional solar cell can only absorb wavelengths up to 1000 nm, but the addition of an upconversion material within the cell (Figure 3a) can increase this range well past 2000 nm.[21]

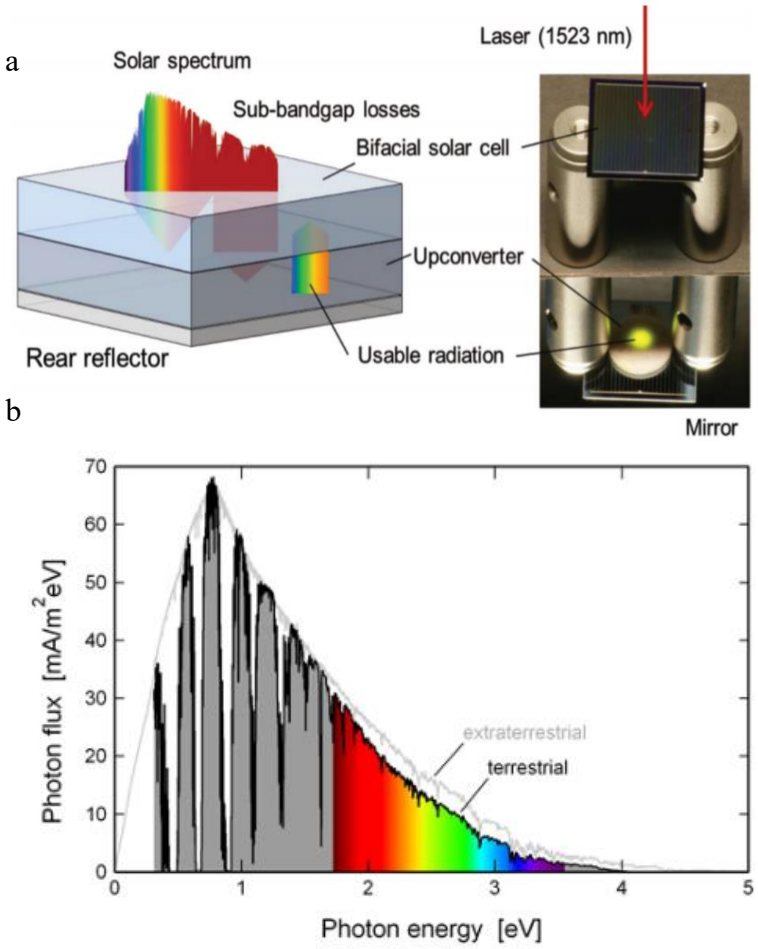

Figure 3. (a) Application of UC in solar energy harvesting and visible light spectrum. (b) Illustration of the photons available in the infrared compared to the visible.[19,21]

Photon upconversion (UC) is a process whereby longer wavelengths of light can be transformed into shorter wavelengths of light that has applications in areas such as bioimaging,[20] nanoparticle materials,[22,23] and as aforementioned, enhanced energy harvesting.[18] Solar panels are generally limited in the range of light that can be transformed into energy, however, utilizing UC to increase the range of available light by transforming uncollected light into a collectable wavelength, increases the overall efficiency of the OPV.[21] There are several mechanisms whereby UC can occur such as energy pooling,[24] two-photon absorption,[25] and photon avalanche,[26] but the utilized mechanism is triplet-triplet annihilation (TTA) due to advantages such as the large anti-Stokes shifts, use of non-coherent light and long triplet lifetimes.[27]

Triplet-triplet annihilation upconversion (TTA-UC) is a process that begins when the sensitizer molecule absorbs energy at the high wavelength, and then enters an excited singlet state. The excited sensitizer then rapidly undergoes a forbidden transition to the triplet state, through intersystem crossing (ISC), promoted by the heavy-atom effect of the palladium metal.[27,28] The excited sensitizer in the triplet state will then undergo triplet-triplet energy transfer (TTET) with an annihilator, exciting the annihilator to the triplet state and relaxing the sensitizer. TTET only occurs when the dyes are within a physical distance (known as the Perrin Limit) of each other allowing for electronic communication.[27] Two annihilator species excited to the triplet state can experience collision and undergo TTA from a higher energy level than initially experienced, therefore emission will produce a higher energy light (Figure 4).[27] An increase in presented energy occurs, but due to the requirement of two initial photons of light that

eventually combine for one higher energy emission, there is a resulting net loss of energy and thus, the first law of thermodynamics is satisfied.

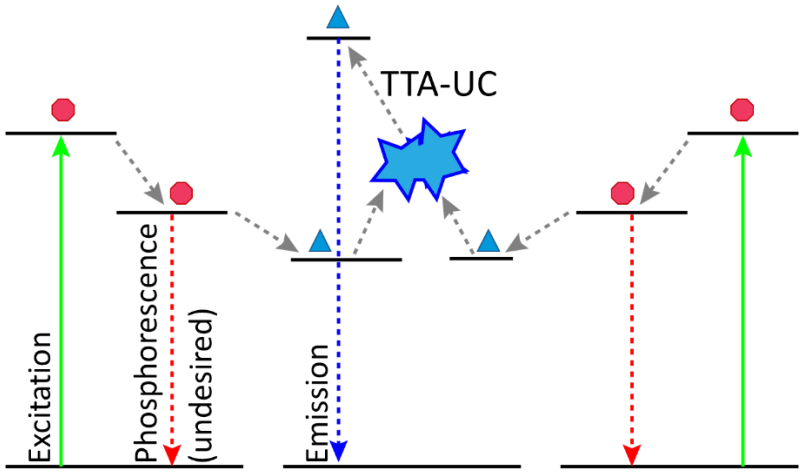

Figure 4. *Illustration of the cascade of the photophysical events of TTA-UC.*

A sensitizer molecule suitable for TTA-UC is typically an inorganic material consisting of a d- or f-block element, and an annihilator species is generally an aromatic hydrocarbon.[27] In the specific system discussed herein, palladium octaethylporphyrin (PdOEP) was used as the sensitizer and 9,10- diphenylanthracene (DPA) as the annihilator (Figure 5). This sensitizer/annihilator pair is often used in literature due to its high quantum yield. Using DPA as the annihilator is known to improve the relative UC yield, due to an increased singlet fluorescence quantum yield, when compared to annihilators like anthracene. The sensitizer PdOEP is used because it obeys the heavy-atom effect, which improves intersystem crossing (ISC) and provides longer triplet excited state that enhances TTET in comparison to other metal complexes.[4,28,29]

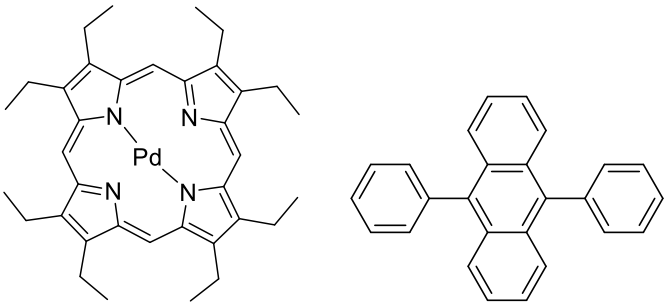

Figure 5. *Chemical structure of PdOEP (sensitizer, left) and DPA (annihilator, right).*

Initially, TTA-UC was only believed possible in solution, where dyes could achieve sufficient diffusion for necessary energy transfers. However, solution-based TTA-UC was impractical due to the vulnerable decay from oxygen that reacts with DPA and inability to be implemented towards applications such as solar cells.[27,30] More recently there have been studies using gels, elastomers, and glassy solids as the matrix for TTA-UC. While gel systems provide the necessary mobility for collisions, they also lend themselves to the aggregation of the highly aromatic dyes.[27] A glassy solid, while relatively inert and more applicable to uses for nanoparticles and solar cells, is often too rigid for each additive to experience collision and TTA-UC is achieved by utilizing a large excess of dyes such that the dyes can experience electronic communication *via* the Perrin limit, which can become costly and inhibit the processing of the polymer.[27] The specific polymer matrix utilized herein (Figure 6) is poly(styrene-isobutylene-styrene) (SIBstar), which is proposed to mediate between these two extremes. SIBstar is a glassy thermodynamic elastomer, a three-armed star block copolymer of poly(isobutylene) (PIB) and poly(styrene) (PS) that experiences phase separation. The rubber properties of PIB (T_g = -73 °C) provide flexibility in the polymer, and the chemical structure permits PIB to act as an oxygen barrier, which is beneficial to reduce degradation of DPA that occurs in

the presence of oxygen.[30] We hypothesized that the dyes will be sequestered in the styrenic portion due to the similarity in aromaticity and structure between DPA and styrene. The dye sequestering will create regions of high dye concentration by preferential dissolution and therefore limit the need for excess addition of dye to promote TTA-UC. Furthermore, utilizing customizable polymer chemistry, the annihilator species can be covalently attached to the glassy PS portion of SIBstar, creating poly(styrene-isobutylene-styrene-DPA) (DPAstar), to further reduce aggregation of this additive.[31]

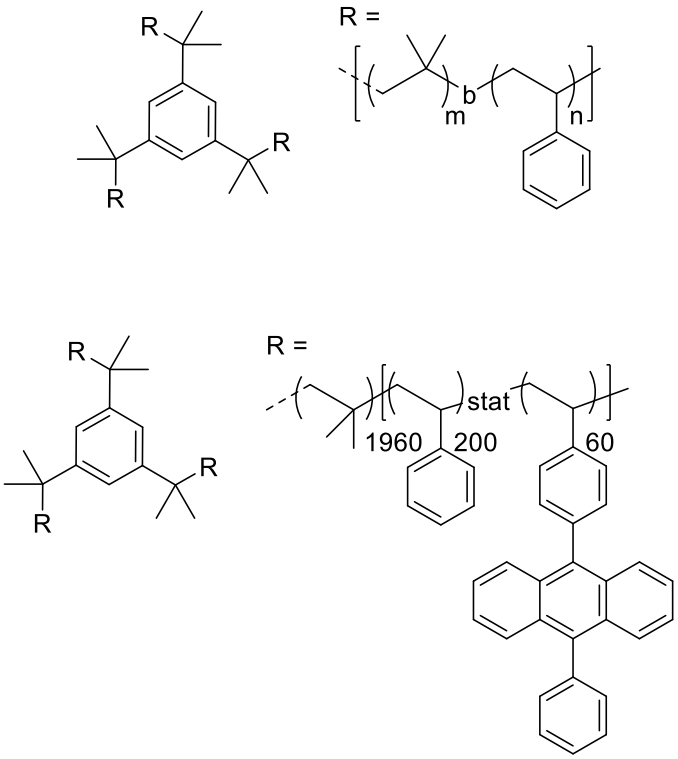

Figure 6. *Chemical structures of SIBstar (top) and DPAstar (bottom).*

Solar energy is the most abundant, and truly renewable, resource available for exploitation. Current technologies, however, can only convert small percentages of solar rays into energy, which reduces the efficiency and increases the cost of resulting solar

panels. Due to an increasing urgency to discover solutions to the energy crisis, the improvement of solar cells is becoming a fast-growing area of research. Upconversion materials provide a pathway that allows a solar cell to increase its efficiency.

CHAPTER II: EXPERIMENTAL

2.1 Materials

All solvents and chemicals were used as received from commercial sources unless otherwise specified. Chloroform, toluene, carbon tetrachloride, chlorobenzene, and dichloromethane were purchased from Fisher Scientific. The dye pair, PdOEP and DPA, was purchased from Frontier Scientific and Oakwood Chemical, respectively. Iron (III) chloride and bromine liquid were purchased from Alfa Aesar. Tetrakis(triphenylphosphine) palladium (0) was purchased from Aldrich Chemistry. Iodine was purchased from Acros. SIBstar (102T, M_n=137 kDa) was purchased from Kaneka. $CDCl_3$ was purchased from Sigma, TCE and DCM were purchased from Cambridge Isotopes for use in NMR.

2.2 Polymer Analysis

2.2.1 Structural Analysis of Polymers

^{1}H NMR was recorded on Varian Mercury 300 MHz spectrometer using $CDCl_3$, TCE, and DCM after each step in the post-polymerization synthesis of DPAstar.

2.2.2 Thermomechanical Analysis of Polymers

TGA was performed on SIBstar and DPAstar via TGA Q500 (TA Instruments, USA) in a platinum pan under a nitrogen atmosphere utilizing a heating ramp at 10 °C min^{-1} from 25 to 800 °C. DSC was performed on both polymer samples via DSC Q100 (TA Instruments, USA) with hermetically sealed aluminum pans, a N_2 atmosphere, and heat/cool/heat cycles at 10 °C min^{-1} from -80 to 280 °C. Each sample was run once.

2.2.3 Optical Analysis of Polymers

UV-Vis was performed on a Lambda 35 UV/Vis Spectrometer (Perkin Elmer, USA) in THF. Photoluminescence measurements were recorded using a PTIHoriba QuantaMaster 400 spectrofluorimeter equipped with a 75 W Xe arc lamp.

2.3 Film Fabrication

2.3.1 Solvent-Casting of Thin Films

DPA (concentration range: 1, 2.5, 5, 15 % w/w DPA/SIBstar), PdOEP (concentration range: 0.5, 0.1, 0.05, 0.025 % w/w PdOEP/SIBstar) and SIBstar (0.8 g) were dissolved in chloroform (10.20 mL) and stirred at 45 °C until homogeneous. Solutions were poured into Teflon evaporating dishes and concentrated at 50 °C in atmospheric conditions for 12 h. Films were then removed from the evaporating dish and dried in a vacuum oven at 60 °C overnight.

2.3.2 Spin-Coating of Thin Films

Spin-coating of thin films were processed using a spinNXG-P1 (Apex Instruments, USA). DPA (concentration range: 15, 25 % w/w DPA/SIBstar), PdOEP (concentration range: 0.1, 0.05 % w/w PdOEP/SIBstar) and SIBstar (0.8 g) were dissolved in chloroform (10.20 mL) and prepared under the same conditions as previously described. A portion of each solution (0.6 mL) was placed on a glass slide and processed at three different rpm settings (2000, 4000, and 6000 rpm).

2.3.3 Melt-Processing of Thin Films

Prior to micro compounding, a film of SIBstar was pressed using a Carver bench top heated press (Carver Inc., USA) under 2 tons of pressure at 240 °C, and the solid dyes were added to the center of the film. It was then folded and pressed again under the same

conditions (Figure 7) before cutting into small pieces that could be added to the pneumatic feeder of the micro compounder in order to avoid adding solids directly to the pneumatic feeder to increase accuracy of w/w calculations of the dyes. Micro compounding of the polymer film blends was carried out with a twin-screw Xplore MC5 (Xplore Instruments, The Netherlands) keeping all heating zones at the set temperature (*vide infra*). Screw rpm was 60 for all blends that were fabricated. Extrudates were pressed using the melt press under 2 tons of pressure at 240 °C. All preliminary films were pressed between Teflon-coated aluminum and removed from the press to cool in atmospheric conditions, and film samples used for optical analysis were pressed between glass slides to allow for easy removal and subsequent quenching in an ice bath.

2.4 Post-Polymerization Modification

2.4.1 Bromination of SIBstar

This reaction was adapted from the literature.[32] SIBstar (15 g, 0.027 mol styrene), ferric chloride (0.266 g, 1.64 mmol), and chloroform (375 mL) were combined in an oven-dried Schlenk vessel (1000 mL) equipped with a reflux condenser and wrapped in foil to protect from light. The brown solution was then sparged with N_2 at room temperature for 45 minutes. A solution of bromine (1.7 mL, 0.032 mol) in $CHCl_3$ (8.5 mL) was added dropwise. The reaction mixture was then heated to reflux overnight. The next day the brown solution was cooled to room temperature and precipitated into methanol to yield a brown solid. The polymer was redissolved in THF and precipitated in MeOH. Due to the persistence of the brown color, the polymer was again dissolved in THF, passed through a basic alumina plug and precipitated into MeOH. The brown solid was then collected *via* filtration and dried overnight *in vacuo* at room temperature.

2.4.2 Suzuki Coupling of DPAstar

A round bottom flask (500 mL) was loaded with bromine functionalized SIBstar **(1)** (9.76 mmol, 1.00 equiv.), (4-(10-phenylanthracen-9-yl)phenyl)boronic acid (14.6 mmol, 1.50 equiv.), tetrabutylammonium bromide (0.976 mmol, 0.10 equiv.), 2 M K_2CO_3 (97.6 mL, 20 equiv.) in water, and anhydrous toluene (100.0 mL). The mixture was sparged with nitrogen, and 40.2 mL of a tetrakis(triphenylphosphine)palladium(0) toluene stock solution (5 mol %) was added dropwise via syringe. The mixture was stirred vigorously and heated conventionally to 100 °C for 24 h before the reaction was allowed to cool, precipitated into MeOH, collected via filtration, and dried in vacuo. The polymer was then redissolved in chlorobenzene and filtered through basic alumina before precipitation into acetone to remove leftover phenyl anthracene boronic acid and dried *in vacuo*. ^{1}H NMR ($CDCl_3$, ppm): δ= 0.87-1.23 (9H, m), 1.23-1.56 (9H, m), 6.00-7.70 (8H, m).

CHAPTER III: RESULTS AND DISCUSSION

3.1 Identification of the Problem

Triplet-triplet based upconversion in the solid state is facilitated either by maintaining dye mobility, or by increasing the concentration of dyes so necessary energy transfer events can occur. In all cases, the dyes must be incorporated into the matrix in a way that prevents aggregation. Aggregation, mainly of the annihilator DPA (due to the requirement of higher concentrations), reduces the efficiency of TTA-UC wherein communication between sensitizer and annihilator is hindered. Uneven distribution of the annihilator is also a result of aggregation that yields an undesirable optical result in the films seen as haziness and a reduction in transparency.

3.2 Solvent-Cast Film Fabrication

3.2.1 Sample Preparation

The initial films for achieving UC in SIBstar were processed by solvent-casting. To ensure the dyes were well dispersed within the matrix, DPA (concentration range: 1, 2.5, 5, 15 % w/w DPA/SIBstar), PdOEP (concentration range: 0.5, 0.1, 0.05, 0.025 % w/w PdOEP/SIBstar) and SIBstar were dissolved in chloroform at 45 °C. Once fully dissolved, the solution was poured into a Teflon dish at 50 °C and left to evaporate in open atmosphere. After 12 h, the films were placed in an oven at 60 °C under vacuum. Using the density of SIBstar (0.954 g/cm^3) and the diameter of the Teflon dish (11 cm), a thickness of 0.2 mm was targeted.

3.2.2 Qualitative Analysis

The films produced *via* solvent-casting were heterogenous in appearance (Figure 8). The thickness of the film varied locally across an individual film. Additionally, while

the films displayed a pink to red hue owing to the incorporation of PdOEP, regions of the film were hazy and opaque, indicating aggregation of DPA. Furthermore, some of the films were heated too quickly, causing the formation of bubbles during the drying process. Overall, these results indicated that the solvent-casting process for this system is very delicate: Fast solvent evaporation is necessary to prevent DPA from aggregating; but overheating can cause solvent bubble formation within the film.

Figure 8. *Solution cast thin film samples of varying dye concentrations.*

3.3 Spin-Coated Film Fabrication and Characterization

3.3.1 Sample Preparation

We transitioned to spin-coating film fabrication to produce films with controllable thickness and eliminate the requirement of heat to avoid bubble production. DPA (concentration range: 15, 25 % w/w DPA/SIBstar), PdOEP (concentration range: 0.1, 0.05 % w/w PdOEP/SIBstar) and SIBstar (0.8 g) were dissolved in chloroform (10.20 mL) at 45 °C. Once fully dissolved, 0.6 mL of solution was placed on a glass slide. Each sample was prepared using 3 rpm settings (2000, 4000, and 6000 rpm) to produce varying

thicknesses where testing could determine the most optimum thickness that could then be easily replicable.

3.3.2 Qualitative Analysis

We assumed that samples fabricated at the same rpm were uniform in thickness, but haziness was still widely present (Figure 9). Optical clarity was achieved after heating the film for 4 hours at 250 °C; the melting temperature of DPA was found *via* DSC. Doing so provided increased mobility for the dyes and allowed the aggregates to disperse evenly throughout the polymer. Reduction of aggregation with heat exemplified the requirement of heat during the processing of TTA-UC films.

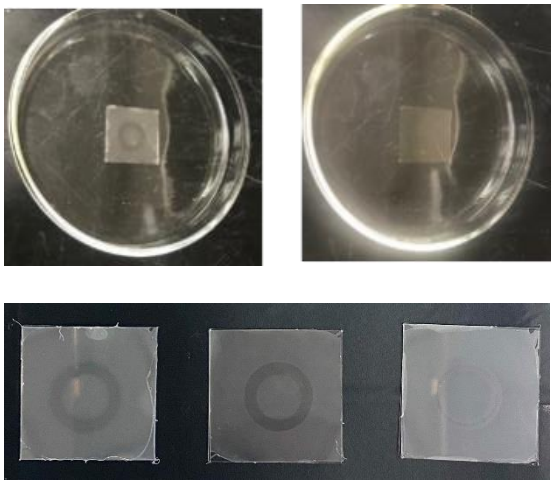

Figure 9. *Spin coated thin film samples of varying dye concentrations.*

3.3.3 Optical Characterization

Spin-coated films were optically characterized by UV-Vis absorbance and photoluminescence experiments (Figure 10). Optical measurements of a film with 0.05 % w/w PdOEP and 25 % w/w DPA at 6000 rpm were analyzed as it exemplified the typical results obtained across all sample types. The absorbance of the spin-coated film showed

excessive scattering and weak signal, though the characteristic vibrational fingerprint of DPA was recognizable. Direct excitation of DPA displayed a strong signal from 360 to 543 nm when excited at 368 nm. Phosphorescence of the sensitizer species was not detected from 625 to 750 nm when excited at 543 nm. Additionally, upconversion was undetectable from 360 to 543 nm when excited at 543 nm, displaying only the upward slope toward 550 nm, which is the interference of incident light. An expected UC signal would appear similar in magnitude and range to that of the direct excitation of DPA. This correlates to a lack of PdOEP in the films, because the photoluminescence data was void of both UC and phosphorescence signals, meaning the problem lies within the lack of sensitizer concentration and does not stem from inefficient communication of the annihilator.

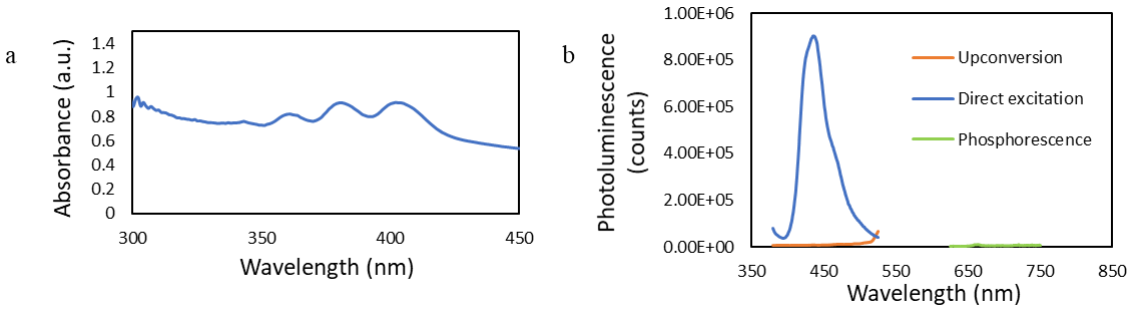

Figure 10. *UV-Vis (a) and PL (b) of a spin-coated film characteristic of all samples made by spin-coating methods.*

3.4 Melt-processed Film Fabrication and Characterization

3.4.1 Sample Preparation

Because it was observed that heat improved clarity in the spin-coated films through removal of aggregation and improved dispersion of dyes within SIBstar, melt-processing was pursued. An initial preliminary film of SIBstar was pressed between

Teflon-coated aluminum on a melt press at 240 °C under 2 tons of pressure for 5 minutes. DPA (concentration range: 5, 10, 25 % w/w DPA/SIBstar), PdOEP (concentration range: 0.1, 0.05 % w/w PdOEP/SIBstar) solids were then added to the preliminary film and the film was folded and pressed again to create a heterogeneously doped polymer film (Figure 11a). The subsequent film was cut into pellet-sized pieces, which were added *via* pneumatic feeder after the micro-compounder reached the processing temperature of 240 °C. Processing of the polymer melt was done for 10 minutes at 60 rpm before extrusion. The flexible extrudate varied in pink hue depending on PdOEP concentration. Small portions of the extrudate were melt-pressed between Teflon-coated aluminum at 240 °C for 5 minutes under 2 tons of pressure to create a homogeneously doped film. Thickness and opacity of the resulting films was undesirable (Figure 11b), as the films had little to no transparency and a pink hue matching the extrudate. Sequential films were pressed between glass slides under the same conditions to achieve greater clarity, and this resulted in films that were optically transparent (Figure 11c).

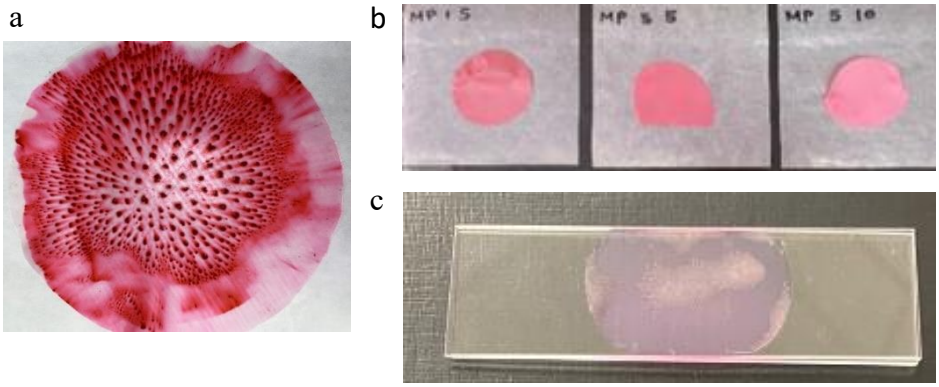

Figure 11. *Melt processed thin film samples of varying dye concentrations. (a) Preliminary film. (b) Films were pressed between sheets of Teflon-coated aluminum and air-cooled. (c) Films were pressed between glass slides and quench-cooled.*

3.4.2 Qualitative Analysis

The utilization of glass slides, rather than Teflon-coated aluminum, provided an additional benefit of quick removal from the melt press, which allowed the film samples to be quenched in an ice bath immediately after pressing. Quench-cooling was done to mitigate the response of aggregation that developed upon letting the films gradually cool to room temperature, by kinetically trapping the dyes in a desirable location within the polymer matrix (Figure 12).

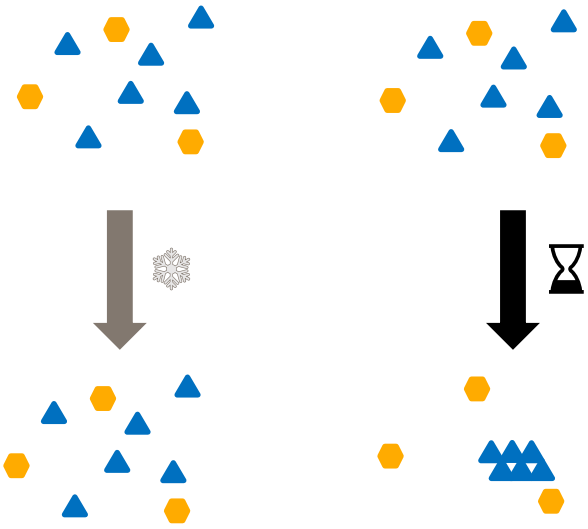

Figure 12. *Illustration of dye placement within the polymer matrix with and without quench cooling.*

3.4.3 Optical Characterization

Optical characterization of the resultant melt-processed films, specifically a film with 0.05 w/w PdOEP and 25 w/w DPA that is representative of other film results, exhibited direct excitation of DPA from 400 to 543 nm and yielded a large signal when excited at 368 nm. Phosphorescence produced a large signal from 600 to 750 nm when excited at 543 nm, which is undesirable as it indicated that PdOEP was incorporated into

the polymer but was not effectively transferring energy to DPA. UC was observable in minute amounts (Figure 13) with a minor curve from 400 to 543 nm when excited at 543 nm. Therefore TTA-UC was prevented either by lack of TTET between PdOEP and DPA, or by ineffective DPA triplet annihilation. In both cases, a probable cause could be aggregation. Because haziness was observed in the films, the next step to reduce aggregation was to covalently attach the annihilator species to the SIBstar backbone.

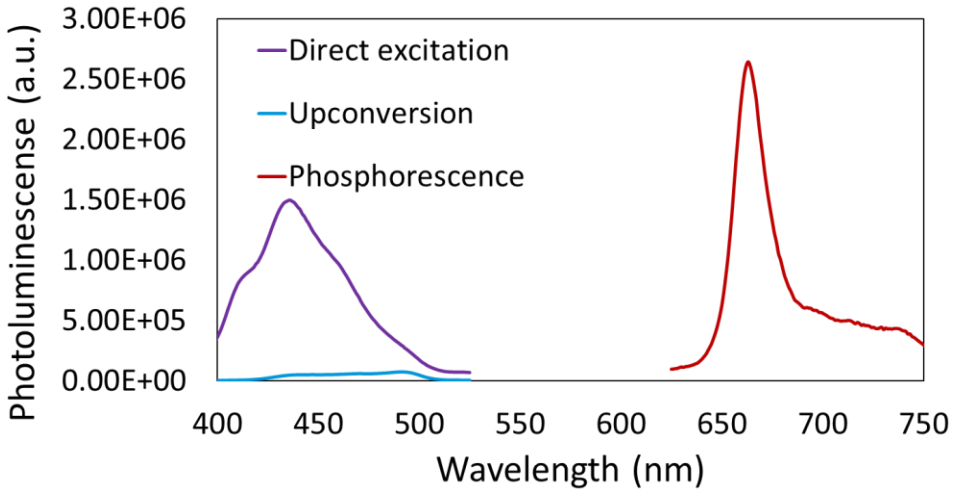

Figure 13. *PL data of melt-processed thin film samples.*

3.5 Post-Polymerization Modification and Characterization

3.5.1 Synthesis

Post-polymerization modification was performed to covalently attach the DPA dye to the backbone of SIBstar to reduce aggregation that was limiting UC (Scheme 1). Modification of the host polymer was achieved *via* bromination and consequent Suzuki coupling reaction. The bromination was performed with SIBstar, liquid bromine, and ferric chloride ($FeCl_3$) in CCl_4 targetting 100% bromination and yielding 50% bromination. A residual brown hue was observed post-bromination, likely due to leftover

bromine, catalytic ferric salts, or other unforseen side products. Precipitation in cold methanol did not reduce this coloration, and it persisted through the Suzuki coupling. The Suzuki reaction was performed with the bromine functionalized SIBstar **(1)**, (4-(10-phenylanthracen-9-yl)phenyl)boronic acid, and tetrakis(triphenylphosphine) palladium(0) as a catalyst. Precipitation in acetone removed excess anthracene and purifies the DPA-modified SIBstar (DPAstar) that was targetted for 50% and yielded 25%.

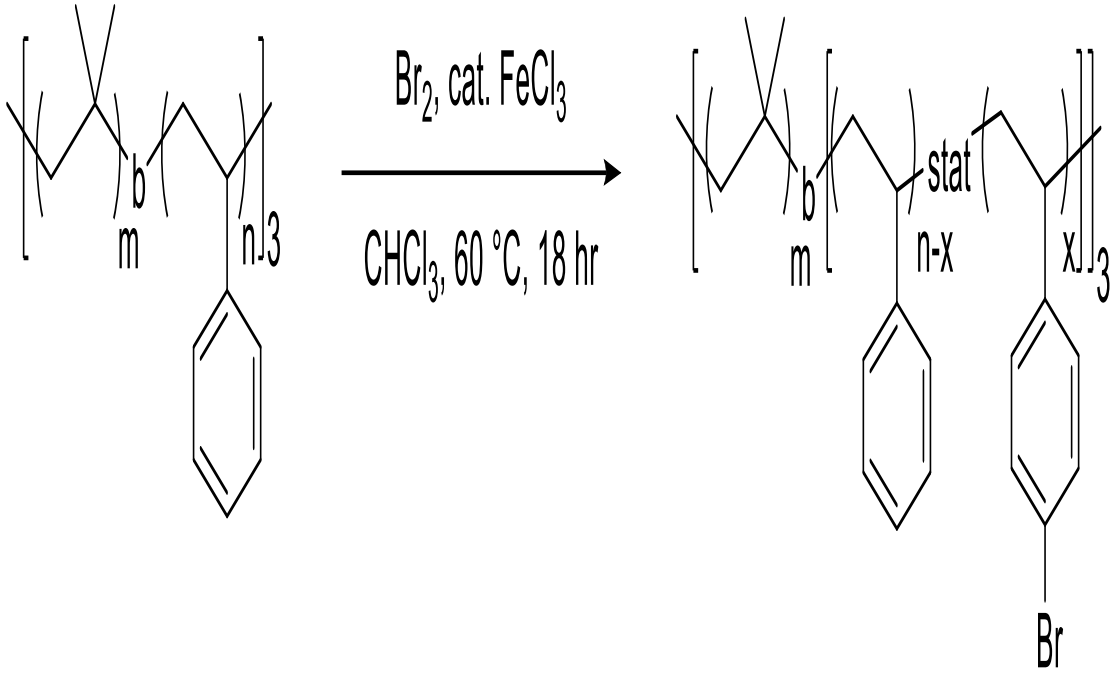

Scheme 1. *Bromination of SIBstar and subsequent Suzuki coupling to yield DPAstar.*

3.5.2 Structural Characterization

Using ^{1}H NMR (Figure 14), DPA was calculated to be attached to the backbone at 25% within the styrenic portion (Equation 1). This calculation can be done by comparing

the aromatic peak in the modified polymer (DPAstar) versus the original (SIBstar). In pristine SIBstar, the ratio of PS to PIB is 1 to 8, which yields a signal ratio of 5 to 18. In DPAstar, when the PIB peak (δ= 1.04 (9H, m), 1.36 (9H, m)) is set to 18, the aromatic peak, now consisting of both the fraction PS (*n*) and DPA (*m*), integrates to 8. Because $n + m = 1$, *m* can be solved for through a system of equations to be 0.25, or 25%. However, there may be discrepancies due to the sharp peaks in the aromatic region which correspond to unreacted anthracene.

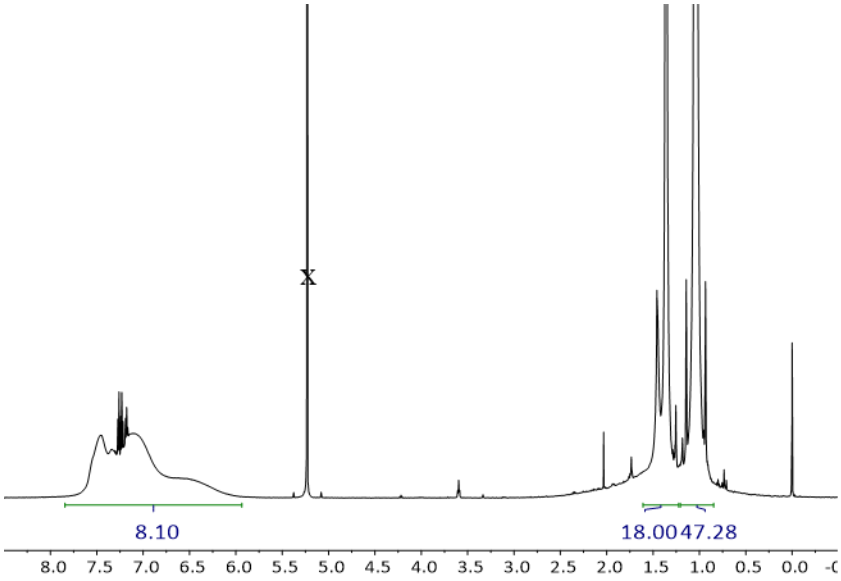

Figure 14. *NMR of DPAstar.*

$$8 = 5n + 17m \quad (1)$$

3.5.3 Thermomechanical Characterization

Thermogravimetric analysis (TGA) of DPAstar (Figure 15) showed that the modified polymer experiences 5% degradation at 330 ℃; therefore the processing temperature used previously, 240 ℃, was still suitable.

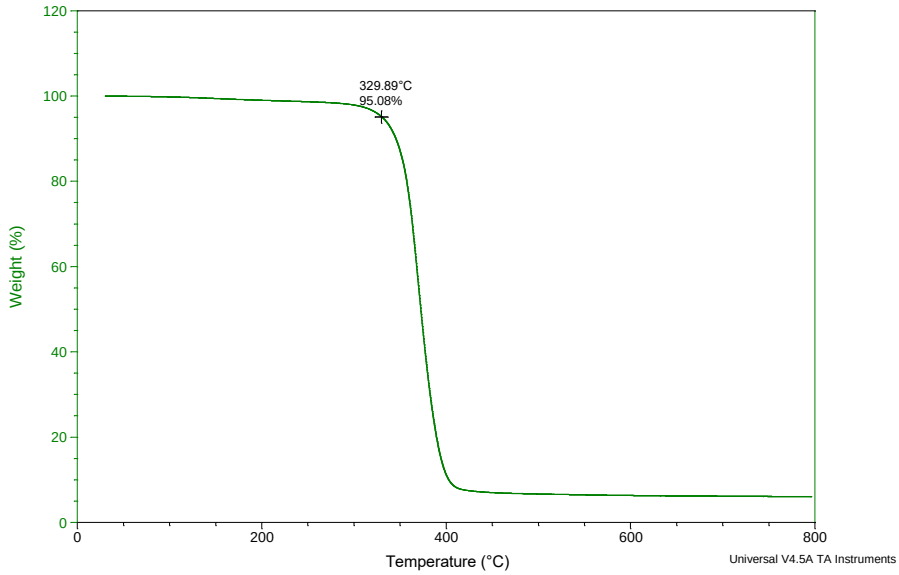

Figure 15. *TGA of DPAstar.*

Further thermomechanical characterization *via* differential scanning calorimetry (DSC) was performed to obtain T_g and, if applicable, melt transition temperature (T_m) of DPAstar. The DSC of DPAstar and SIBstar in Figure 16 shows overwhelming similarity between the two polymers, barring a small melting peak at 250 °C which is likely from the T_m of DPA and further implies aggregation of the dye within the polymer. The cooling system utilized with this instrument cannot accurately cool past -80 °C, and therefore the T_g of PIB could not be assessed. The large peak from -50 to 100 °C is likely due to an entropic effect. One could further assume that melt processing parameters would be transferrable to the modified polymer.

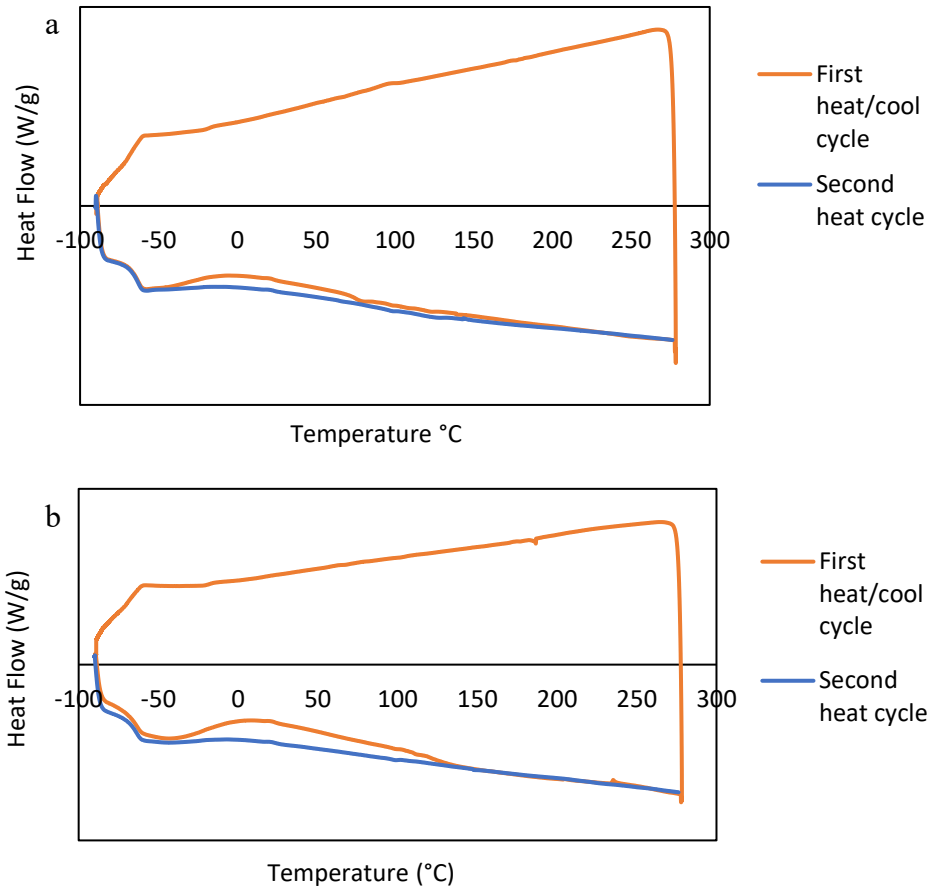

Figure 16. *DSC of (a) SIBstar and (b) DPAstar.*

3.5.4 Optical Characterization

Optical characterization was performed on DPA and DPAstar to compare the relationships between the annihilator as a dye and as a part of the polymer backbone. Initially, UV-Vis of each dye, and DPAstar were plotted as absorbance vs. wavelength (Figure 17) to confirm the concentration of the dye within the modified polymer. DPAstar has a similar signal as DPA with three distinctive peaks. This is expected due to the presence of the dye within the polymer, though the DPAstar absorbance signal is

much weaker than that of DPA as the dye is less concentrated within the polymer. The signal for PdOEP is provided for reference.

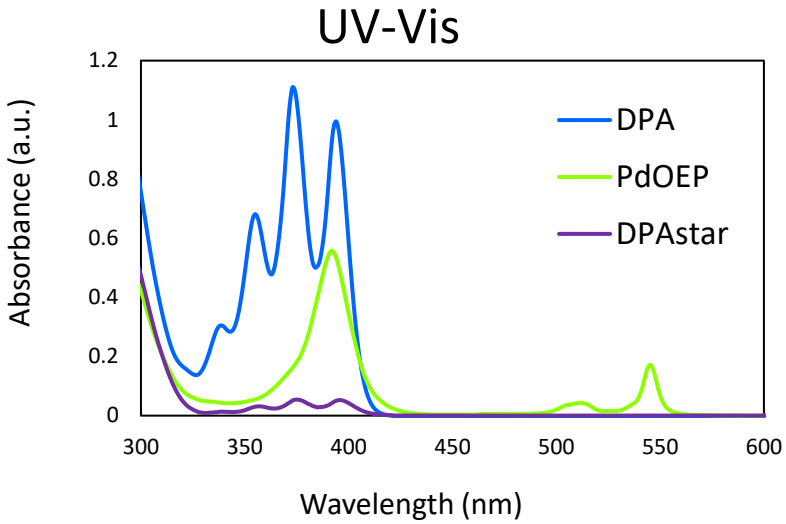

Figure 17. *UV-Vis of dyes and DPAstar*.

Utilizing Beer-Lambert's Law (Equation 2), the moles of DPA present in the modified polymer can be determined. In this equation, A is absorbance, b is the path length (1 cm), c is concentration of the sample, and ε is the molar absorptivity that can be found from the slope of a concentration vs. absorbance plot (Figure 18). The molar quantity of DPA was found to be 0.05438, and the mol% of DPA in the polymer was calculated to be 10.51% by weight. This falls short of the value of 25 wt% determined by NMR, which is likely due to the deterioration of the solubility of DPAstar over time.

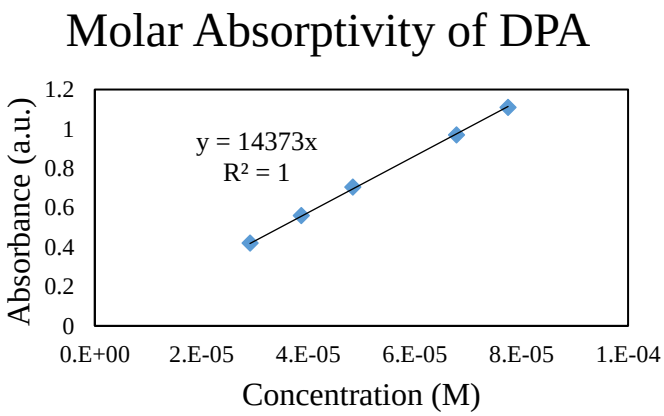

Figure 18. *Molar absorbance plot of DPA solutions at various concentrations.*

$$A = \varepsilon * b * c \quad (2)$$

3.6 Melt-Pressed Modified Film Fabrication

Difficulties persisted when attempting to melt process DPAstar. Comparison of SIBstar and DPAstar after melt pressing in the same conditions (240 °C, 2 tons, 5 minutes) displays vast differences between the pristine polymer and the modified polymer (Figure 19). The ripping and degradation of DPAstar gives reason to believe that crosslinking had occurred within the polymer overt ime, and this rendered it unable to be processed, which was further confirmed by the decreasing solubility in the polymer over time.

a 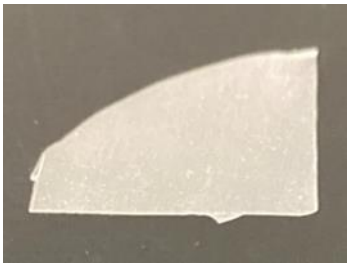 b 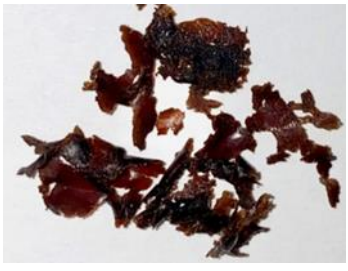

Figure 19*. SIBstar (a) and DPAstar (b) samples after melt processing.*

CHAPTER IV: CONCLUSION

Thermoplastic elastomers demonstrate great potential in housing TTA-UC mechanisms that provide adequate mobility of annihilator and sensitizer species within the matrix. Film fabrication was performed by multiple methods consisting of solution-casting, spin-coating, and melt-pressing. UV-Vis and PL spectra show minor UC signals seen only in melt-pressed films of SIBstar when doped with PdOEP and DPA. ^{1}H NMR confirmed initial success of a post-polymerization modification of SIBstar to covalently attach DPA within the PS phase of the polymer backbone. The subsequent polymer, DPAstar, displayed similar thermomechanical properties to the unmodified polymer *via* TGA and DSC, but overtime DPAstar became increasingly unprocessible by previous melt processing methodologies, likely due to undesired crosslinking. As a result, optical characterization was difficult to obtain in the solid state, but solution state samples displayed little to know improvement in TTA-UC within the modified host polymer.

REFERENCES

(1) Wong, W. Y.; Ho, C. L.; Wong, Wai-Yeung; Ho, C. Organometallic Photovoltaics : A New and Versatile Approach for Harvesting Solar Energy Using Conjugated Polymetallaynes. *Acc. Chem. Res.* **2010**, *43* (9), 1246–1259.

(2) Murdock, H. E.; Gibb, D.; André, T. *Renewables 2019 Global Status Report*; **2019**; Vol. 8.

(3) Capuano, L. U. S. Energy Information Administration's International Energy Outlook 2020. *Https://Www.Eia.Gov/Outlooks/Ieo/* **2020**.

(4) Lewis, N. S.; Crabtree, G. Basic Research Needs for Solar Energy Utilization. *https://science.osti.gov/~/media/bes/pdf/reports/files/Basic_Research_Needs_for_Solar_Energy_Utilization_rpt.pdf* **2005**.

(5) Guo, X.; Liu, Y.; Chen, Q.; Zhao, D.; Ma, Y. New Bichromophoric Triplet Photosensitizer Designs and Their Application in Triplet–Triplet Annihilation Upconversion. *Adv. Opt. Mater.* **2018**, *6* (4), 1–16.

(6) Alhalafi, A. Applications of Polymers in Intraocular Drug Delivery Systems. *Oman Journal of Ophthalmology*. Medknow Publications January 1, **2017**, pp 3–8.

(7) Teles, F. R. R.; Fonseca, L. P. Applications of Polymers for Biomolecule Immobilization in Electrochemical Biosensors. *Materials Science and Engineering C*. Elsevier December 1, **2008**, pp 1530–1543.

(8) Cui, Y.; Yao, H.; Zhang, J.; Xian, K.; Zhang, T.; Hong, L.; Wang, Y.; Xu, Y.; Ma, K.; An, C.; He, C.; Wei, Z.; Gao, F.; Hou, J. Single-Junction Organic Photovoltaic Cells with Approaching 18% Efficiency. *Adv. Mater.* **2020**, *32* (19), 1–7.

(9) Hou, W.; Xiao, Y.; Han, G.; Lin, J.-Y. The Applications of Polymers in Solar

Cells: A Review. *Polymers (Basel).* **2019**, *11* (1), 143.

(10) Wu, Y.; An, C.; Shi, L.; Yang, L.; Qin, Y.; Liang, N.; He, C.; Wang, Z.; Hou, J. The Crucial Role of Chlorinated Thiophene Orientation in Conjugated Polymers for Photovoltaic Devices. *Angew. Chemie Int. Ed.* **2018**, *57* (39), 12911–12915.

(11) Holliday, S.; Li, Y.; Luscombe, C. K. Recent Advances in High Performance Donor-Acceptor Polymers for Organic Photovoltaics. *Progress in Polymer Science*. **2017**, pp 34–51.

(12) Antohe, S.; Iftimie, S.; Hrostea, L.; Antohe, V. A.; Girtan, M. A Critical Review of Photovoltaic Cells Based on Organic Monomeric and Polymeric Thin Film Heterojunctions. *Thin Solid Films*. **2017**, pp 219–231.

(13) Goldschmidt, J. C.; Fischer, S. Upconversion for Photovoltaics - a Review of Materials, Devices and Concepts for Performance Enhancement. *Adv. Opt. Mater.* **2015**, *3* (4), 510–535.

(14) Nattestad, A.; Cheng, Y. Y.; Macqueen, R. W.; Schulze, T. F.; Thompson, F. W.; Mozer, A. J.; Fückel, B.; Khoury, T.; Crossley, M. J.; Lips, K.; Wallace, G. G.; Schmidt, T. W. Dye-Sensitized Solar Cell with Integrated Triplet-Triplet Annihilation Upconversion System. *J. Phys. Chem. Lett.* **2013**, *4* (12), 2073–2078.

(15) Liu, Q.; Yang, T.; Feng, W.; Li, F. Blue-Emissive Upconversion Nanoparticles for Low-Power-Excited Bioimaging in Vivo. *J. Am. Chem. Soc.* **2012**, *134* (11), 5390–5397.

(16) van Sark, W. G. J. H. M.; Meijerink, A.; Schropp, R. E. I. Solar Spectrum Conversion for Photovoltaics Using Nanoparticles. *Third Generation Photovoltaics*. **2012**. DOI: 10.5772/39213

(17) Liu, X.; Yan, C. H.; Capobianco, J. A. Photon Upconversion Nanomaterials. *Chemical Society Reviews*. **2015**, pp 1299–1301.

(18) Wang, M.; Abbineni, G.; Clevenger, A.; Mao, C.; Xu, S. Upconversion Nanoparticles: Synthesis, Surface Modification and Biological Applications. *Nanomedicine: Nanotechnology, Biology, and Medicine*. **2011**, pp 710–729.

(19) Weingarten, D. H.; Lacount, M. D.; Van De Lagemaat, J.; Rumbles, G.; Lusk, M. T.; Shaheen, S. E. Experimental Demonstration of Photon Upconversion via Cooperative Energy Pooling. *Nat. Commun.* **2017**, *8*, 4–10.

(20) Ha, H. D.; Jang, M. H.; Liu, F.; Cho, Y. H.; Seo, T. S. Upconversion Photoluminescent Metal Ion Sensors via Two Photon Absorption in Graphene Oxide Quantum Dots. *Carbon N. Y.* **2015**, *81* (1), 367–375.

(21) Lahoz, F.; Martín, I. R.; Calvilla-Quintero, J. M. Ultraviolet and White Photon Avalanche Upconversion in Ho3+ -Doped Nanophase Glass Ceramics. *Appl. Phys. Lett.* **2005**, *86* (5), 1–3.

(22) Simon, Y. C.; Weder, C. Low-Power Photon Upconversion through Triplet-Triplet Annihilation in Polymers. *J. Mater. Chem.* **2012**, *22* (39), 20817–20830.

(23) Islangulov, R. R.; Kozlov, D. V.; Castellano, F. N. Low Power Upconversion Using MLCT Sensitizers. *Chem. Commun.* **2005**, *1* (30), 3776–3778.

(24) Zhao, J.; Ji, S.; Guo, H. Triplet-Triplet Annihilation Based Upconversion: From Triplet Sensitizers and Triplet Acceptors to Upconversion Quantum Yields. *RSC Adv.* **2011**, *1* (6), 937–950.

(25) Filatov, M. A.; Heinrich, E.; Busko, D.; Ilieva, I. Z.; Landfester, K.; Baluschev, S.

Reversible Oxygen Addition on a Triplet Sensitizer Molecule: Protection from Excited State Depopulation. *Phys. Chem. Chem. Phys.* **2015**, *17* (9), 6501–6510.